Special Green's function boundary element approach for steady-state axisymmetric heat conduction across low and high conducting planar interfaces*

E. L. Chen and W. T. Ang
Division of Engineering Mechanics
School of Mechanical and Aerospace Engineering
Nanyang Technological University
Republic of Singapore

Abstract

The problem of determining the steady-state axisymmetric temperature distribution in a bimaterial with a planar interface is considered here. The interface is either low or high conducting. Special Green's functions satisfying the thermal conditions on the interface are derived and employed to obtain boundary integral equations whose path of integration does not include the interface. Boundary element procedures that do not require the interface to be discretized into elements are proposed for solving the problem under consideration.

Keywords: Green's functions, bimaterial, low and high conducting interfaces, boundary element method.

* Preprint of article to appear in *Applied Mathematical Modelling*. For details, visit http://dx.doi.org/10.1016/j.apm.2012.04.051

1 Introduction

Two dissimilar materials bonded together with a very thin layer of material sandwiched in between them may be modeled as a bimaterial with an interface in the form of a line (for plane problems) or a surface (for three-dimensional problems). For heat conduction problems, the thermal conditions to impose on the line or surface interface depend on the thermal conductivity of the thin layer and may be derived using the asymptotic analysis in Benveniste [1].

If the temperature and the normal heat flux are continuous on the interface, it (the interface) is considered as ideal (perfect). If the thin (interphase) layer has an extremely low thermal conductivity, the layer may be modeled as an interface over which the temperature is discontinuous. Such an interface is said to be thermally low conducting. For example, the interface between two imperfectly joined solids may be modeled as low conducting if it contains microscopic gaps filled with air. On the other extreme, the thin layer may be modeled as a high conducting interface with discontinuous normal heat flux if the layer is occupied by a material of high thermal conductivity such as carbon nanotubes (Desai *et al* [2]).

Some Green's functions for steady-state heat conduction across planar interfaces between dissimilar materials may be found in the literature. A Green's function for two-dimensional heat conduction across an ideal interface between two thermally anisotropic half-spaces was used in Berger and Karageorghis [3] to develop a meshless method for analyzing the temperature distribution in a bimaterial. Ang *et al* [4] derived a Green's function for two-dimensional heat conduction across a low conducting interface between two thermally isotropic half-spaces. The Green's function was applied to derive boundary element procedures for solving two-dimensional heat conduction problems involving bimaterials of finite extent (see also Ang [5]). Three-dimensional Green's functions for heat conduction across low and high conducting interfaces were given in Wang and Sudak [6].

In the present paper, we consider the problem of determining the steady-state axisymmetric temperature distribution in an axisymmetric bimaterial with a planar interface which is either low or high conducting. For thermal analysis of the bimaterial, special Green's functions satisfying the relevant thermal conditions on the interface are derived and employed to obtain boundary integral equations whose path of integration does not include the interface. Boundary element procedures that do not require the interface to be discretized into elements are proposed. To check the validity and accuracy of the boundary element procedures, they are applied to solve some specific problems.

2 The problem

Consider two dissimilar materials bonded together with a thin layer of material sandwiched in between them. The regions occupied by the layer and the two dissimilar materials are denoted by R_0, R_1 and R_2 respectively. With reference to a Cartesian coordinate system denoted by $Oxyz$, R_0 occupies part of the space $-h/2 < z < h/2$, where h is a given positive number. The regions R_1 and R_2 are subsets of the half-spaces $z < -h/2$ and $z > h/2$ respectively. The regions R_0, R_1 and R_2 are axisymmetric, obtained by rotating respectively two-dimensional regions Ω_0, Ω_1 and Ω_2 on the Orz (axisymmetric coordinate) plane (as sketched in Figure 1) by an angle of 360^{o} about the z-axis. Note that r is the distance of a point from the z-axis.

The thermal conductivities of the materials in Ω_0, Ω_1 and Ω_2 are positive constants κ_0, κ_1 and κ_2 respectively. We are interested in modeling the sandwiched layer Ω_0 as a line interface on the z-axis of the Orz plane for the limiting case in which the thickness h tends to zero. A geometrical sketch of the body with the line interface $a < r < b$, $z = 0$ denoted by Γ_0 is shown in Figure 2. (Note that the constant a is 0 if Ω_0 and Γ_0 are as sketched in Figures 1 and 2 respectively. In general, depending on the geometries of Ω_0, Ω_1 and Ω_2, a is not necessarily zero.) The asymptotic approach in Benveniste [1] may be employed to derive appropriate thermal conditions to impose on the line interface Γ_0.

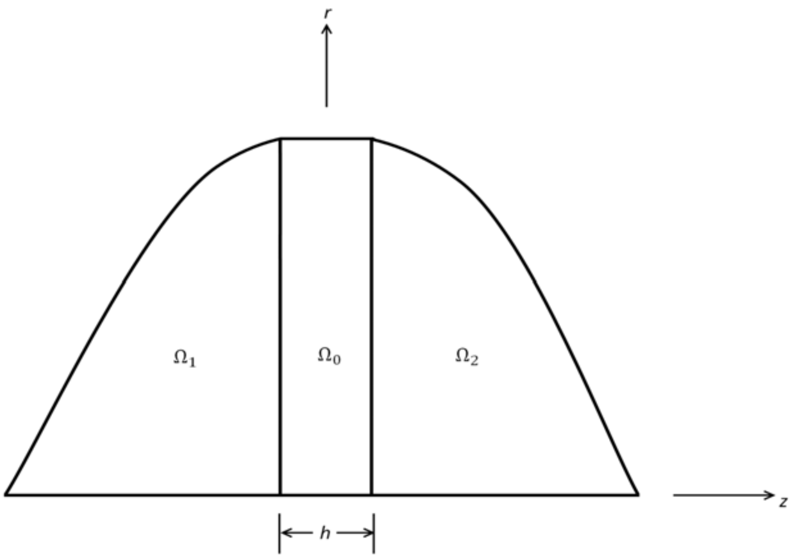

Figure 1. The regions Ω_0, Ω_1 and Ω_2 are rotated by an angle of $360^{\rm o}$ about the z-axis to form the three-dimensional regions R_0, R_1 and R_2 respectively.

It is assumed here that the temperature in the materials is steady and varies spatially with the axisymmetric coordinates r and z only. Denoted by $T(\underline{\mathbf{x}})$ (where $\underline{\mathbf{x}} = (r, z)$), the temperature satisfies the governing partial differential equation

$$\frac{\partial^2 T}{\partial r^2} + \frac{1}{r}\frac{\partial T}{\partial r} + \frac{\partial^2 T}{\partial z^2} = 0 \quad \text{for } \underline{\mathbf{x}} \in \Omega_0 \cup \ \Omega_1 \cup \Omega_2. \tag{1}$$

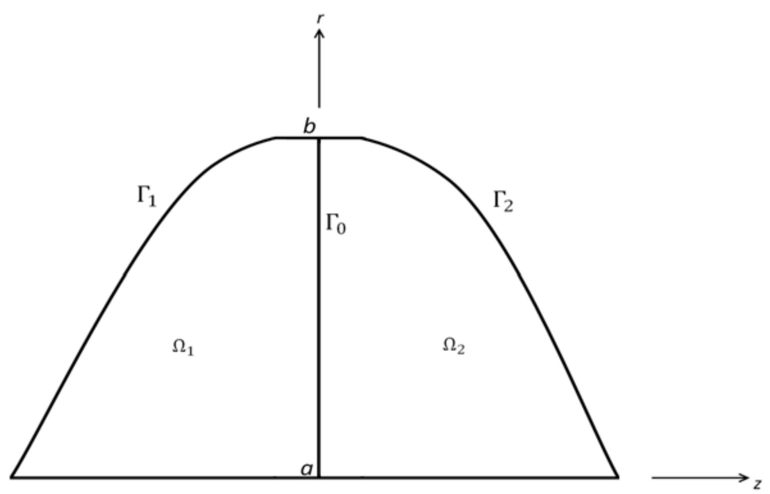

Figure 2. The layer Ω_0 is replaced by the line Γ_0 as h tends to zero. Apart from Γ_0, the curves Γ_1 and Γ_2 make up the remaining boundaries of Ω_1 and Ω_2 respectively.

The line interface Γ_0 between Ω_1 and Ω_2 in Figure 2 is said to be ideal or perfectly conducting if the temperature T and the normal heat flux are continuous on Γ_0, that is, if the thermal conditions on the interface are given by

$$\left.\begin{aligned} T(r,0^+) &= T(r,0^-) \\ \kappa_2 \left.\frac{\partial T}{\partial z}\right|_{z=0^+} &= \kappa_1 \left.\frac{\partial T}{\partial z}\right|_{z=0^-} \end{aligned}\right\} \text{for } \ a < r < b. \tag{2}$$

If the thermal conductivity κ_0 in the layer Ω_0 is such that

$$\frac{\kappa_0}{h} \to \lambda \text{ (a finite positive constant) as } h \to 0^+, \tag{3}$$

then the asymptotic analysis in Benveniste [1] may be used to derive the following thermal conditions on Γ_0:

$$\left.\begin{aligned} \kappa_2 \left.\frac{\partial T}{\partial z}\right|_{z=0^+} &= \kappa_1 \left.\frac{\partial T}{\partial z}\right|_{z=0^-} \\ \lambda[T(r,0^+) - T(r,0^-)] &= \kappa_2 \left.\frac{\partial T}{\partial z}\right|_{z=0^+} \end{aligned}\right\} \text{for } \ a < r < b. \tag{4}$$

Note that (3) implies that κ_0 approaches zero as h tends to zero. Thus, (4) gives the thermal conditions on a layer with thickness and thermal conductivity that tend to zero in such a way that there is a temperature jump across opposite sides of the layer of vanishing thickness. A non-ideal conducting interface with such thermal conditions is said to be low conducting. The line interface Γ_0 between two materials as sketched in Figure 2 may be modeled as low conducting if the interface is imperfect containing microscopic gaps filled with air.

For another non-ideal conducting interface, if the thermal conductivity of the layer Ω_0 is given by

$$\kappa_0 h \to \alpha \text{ (a finite positive constant) as } h \to 0^+, \tag{5}$$

then the thermal conditions on Γ_0 are given by

$$\left.\begin{aligned} T(r,0^+) &= T(r,0^-) \\ \kappa_2 \left.\frac{\partial T}{\partial z}\right|_{z=0^+} - \kappa_1 \left.\frac{\partial T}{\partial z}\right|_{z=0^-} &= \alpha \left.\frac{\partial^2 T}{\partial z^2}\right|_{z=0} \end{aligned}\right\} \text{for } \ a < r < b. \tag{6}$$

In view of the first condition in (6) and the governing partial differential equation in (1), note that

$$\begin{aligned}\left.\frac{\partial^2 T}{\partial z^2}\right|_{z=0^+} &= -\left.\frac{1}{r}\frac{\partial}{\partial r}(r\frac{\partial T}{\partial r})\right|_{z=0^+} \\ &= -\left.\frac{1}{r}\frac{\partial}{\partial r}(r\frac{\partial T}{\partial r})\right|_{z=0^-} = \left.\frac{\partial^2 T}{\partial z^2}\right|_{z=0^-}.\end{aligned} \tag{7}$$

As implied by (5), the thermal conductivity κ_0 in the layer Ω_0 tends to infinity as h vanishes. Thus, a non-ideal conducting interface with the thermal conditions (6) in which the normal heat flux is discontinuous across the vanishing interphase layer is said to be high conducting. For a practical example, if the two materials in Figure 2 are joined together by an extremely thin layer of carbon nanotubes, the line interface may be modeled as high conducting.

The problem of interest here is to solve (1) for the axisymmetric steady-state temperature in the bimaterial sketched in Figure 2, that is, in $\Omega_1 \cup \Omega_2$, subject to either (4) or (6) (as the thermal conditions on Γ_0) and suitably prescribed temperature or flux at each point on the exterior boundary $\Gamma_1 \cup \Gamma_2$ of the bimaterial. Specifically, the boundary conditions on $\Gamma_1 \cup \Gamma_2$ are given by

$$\begin{aligned} T(\underline{\mathbf{x}}) &= f_0(\underline{\mathbf{x}}) \text{ for } \underline{\mathbf{x}} \in \Xi_1, \\ P(\underline{\mathbf{x}}; \underline{\mathbf{n}}(\underline{\mathbf{x}})) &= f_1(\underline{\mathbf{x}}) + f_2(\underline{\mathbf{x}})T(\underline{\mathbf{x}}) \text{ for } \underline{\mathbf{x}} \in \Xi_2, \end{aligned} \tag{8}$$

where $f_0(\underline{\mathbf{x}})$, $f_1(\underline{\mathbf{x}})$ and $f_2(\underline{\mathbf{x}})$ are suitably prescribed functions, Ξ_1 and Ξ_2 are non-intersecting curves (for the different boundary conditions) such that $\Xi_1 \cup \Xi_2 = \Gamma_1 \cup \Gamma_2$.

3 Green's function boundary element method

3.1 Boundary integral equations

The boundary integral equations for axisymmetric heat conduction governed by (1) in the bimaterial sketched in Figure 2 are given by (see Brebbia *et al* [7])

$$\begin{aligned}
&\gamma_1(\underline{\mathbf{x}}_0)T(\underline{\mathbf{x}}_0) \\
&= \int\limits_{\Gamma_1} (T(\underline{\mathbf{x}})G_1(\underline{\mathbf{x}};\underline{\mathbf{x}}_0;\underline{\mathbf{n}}(\underline{\mathbf{x}})) - G_0(\underline{\mathbf{x}};\underline{\mathbf{x}}_0)P(\underline{\mathbf{x}};\underline{\mathbf{n}}(\underline{\mathbf{x}})))r ds(\underline{\mathbf{x}}) \\
&+ \int_a^b (T(r,0^-)G_1(r,0^-;\underline{\mathbf{x}}_0;0,1) - G_0(r,0^-;\underline{\mathbf{x}}_0)\,\frac{\partial}{\partial z}[T(\underline{\mathbf{x}})]\bigg|_{z=0^-})r dr \\
&\qquad\qquad\qquad \text{for } \underline{\mathbf{x}}_0 = (r_0, z_0) \in \Omega_1 \cup \Gamma_0 \cup \Gamma_1,
\end{aligned} \tag{9}$$

and

$$\begin{aligned}
&\gamma_2(\underline{\mathbf{x}}_0)T(\underline{\mathbf{x}}_0) \\
&= \int\limits_{\Gamma_2} (T(\underline{\mathbf{x}})G_1(\underline{\mathbf{x}};\underline{\mathbf{x}}_0;\underline{\mathbf{n}}(\underline{\mathbf{x}})) - G_0(\underline{\mathbf{x}};\underline{\mathbf{x}}_0)P(\underline{\mathbf{x}};\underline{\mathbf{n}}(\underline{\mathbf{x}})))r ds(\underline{\mathbf{x}}) \\
&- \int_a^b (T(r,0^+)G_1(r,0^+;\underline{\mathbf{x}}_0;0,1) - G_0(r,0^+;\underline{\mathbf{x}}_0)\,\frac{\partial}{\partial z}[T(\underline{\mathbf{x}})]\bigg|_{z=0^+})r dr \\
&\qquad\qquad\qquad \text{for } \underline{\mathbf{x}}_0 \in \Omega_2 \cup \Gamma_0 \cup \Gamma_2,
\end{aligned} \tag{10}$$

where $\gamma_i(\underline{\mathbf{x}}_0) = 1$ if $\underline{\mathbf{x}}_0$ lies in the interior of Ω_i, $\gamma_1(\underline{\mathbf{x}}_0)$ and $\gamma_2(\underline{\mathbf{x}}_0)$ are defined by

$$\begin{aligned}
\gamma_1(\underline{\mathbf{x}}_0) = \int\limits_{\Gamma_1} G_1(\underline{\mathbf{x}};\underline{\mathbf{x}}_0;\underline{\mathbf{n}}(\underline{\mathbf{x}}))r ds(\underline{\mathbf{x}}) + \int_a^b G_1(r,0^-;\underline{\mathbf{x}}_0;0,1)r dr \\
\text{for } \underline{\mathbf{x}}_0 = (r_0, z_0) \in \Omega_1 \cup \Gamma_0 \cup \Gamma_1,
\end{aligned} \tag{11}$$

and

$$\gamma_2(\underline{\mathbf{x}}_0) = \int\limits_{\Gamma_2} G_1(\underline{\mathbf{x}};\underline{\mathbf{x}}_0;\underline{\mathbf{n}}(\underline{\mathbf{x}}))rds(\underline{\mathbf{x}}) - \int_a^b G_1(r,0^+;\underline{\mathbf{x}}_0;0,1)rdr$$

$$\text{for } \underline{\mathbf{x}}_0 \in \Omega_2 \cup \Gamma_0 \cup \Gamma_2, \tag{12}$$

$ds(\underline{\mathbf{x}})$ denotes the length of an infinitesimal part of the curve $\Gamma_0 \cup \Gamma_i$, $\underline{\mathbf{n}}(\underline{\mathbf{x}}) = [n_r(\underline{\mathbf{x}}), n_z(\underline{\mathbf{x}})] = n_r(\underline{\mathbf{x}})\underline{\mathbf{e}}_r + n_z(\underline{\mathbf{x}})\underline{\mathbf{e}}_z$ ($\underline{\mathbf{e}}_r$ and $\underline{\mathbf{e}}_z$ are the unit base vectors along the r and z axes respectively) is the unit normal vector to $\Gamma_1 \cup \Gamma_2$ (at the point $\underline{\mathbf{x}}$) pointing out of $\Omega_1 \cup \Omega_2$, $P(\underline{\mathbf{x}};\underline{\mathbf{n}}(\underline{\mathbf{x}}))$ is the directional rate of change of the axisymmetric temperature along the vector $\underline{\mathbf{n}}(\underline{\mathbf{x}})$ as defined by

$$P(\underline{\mathbf{x}};\underline{\mathbf{n}}(\underline{\mathbf{x}})) = n_r(\underline{\mathbf{x}})\frac{\partial}{\partial r}[T(\underline{\mathbf{x}})] + n_z(\underline{\mathbf{x}})\frac{\partial}{\partial z}[T(\underline{\mathbf{x}})], \tag{13}$$

and $G_0(\underline{\mathbf{x}};\underline{\mathbf{x}}_0)$ and $G_1(\underline{\mathbf{x}};\underline{\mathbf{x}}_0;\underline{\mathbf{n}}(\underline{\mathbf{x}}))$ are given by

$$\begin{aligned}
G_0(\underline{\mathbf{x}};\underline{\mathbf{x}}_0) &= [H(z)H(z_0) + H(-z)H(-z_0)]G_0^{(1)}(\underline{\mathbf{x}};\underline{\mathbf{x}}_0) + G_0^{(2)}(\underline{\mathbf{x}};\underline{\mathbf{x}}_0),\\
G_1(\underline{\mathbf{x}};\underline{\mathbf{x}}_0;\underline{\mathbf{n}}(\underline{\mathbf{x}})) &= [H(z)H(z_0) + H(-z)H(-z_0)]G_1^{(1)}(\underline{\mathbf{x}};\underline{\mathbf{x}}_0;\underline{\mathbf{n}}(\underline{\mathbf{x}}))\\
&\quad + G_1^{(2)}(\underline{\mathbf{x}};\underline{\mathbf{x}}_0;\underline{\mathbf{n}}(\underline{\mathbf{x}})),\\
G_0^{(1)}(\underline{\mathbf{x}};\underline{\mathbf{x}}_0) &= -\frac{K(m(\underline{\mathbf{x}};\underline{\mathbf{x}}_0))}{\pi\sqrt{a(\underline{\mathbf{x}};\underline{\mathbf{x}}_0) + b(r;r_0)}},\\
G_1^{(1)}(\underline{\mathbf{x}};\underline{\mathbf{x}}_0;\underline{\mathbf{n}}(\underline{\mathbf{x}})) &= -\frac{1}{\pi\sqrt{a(\underline{\mathbf{x}};\underline{\mathbf{x}}_0) + b(r;r_0)}}\\
&\quad \times \{\frac{n_r(\underline{\mathbf{x}})}{2r}[\frac{r_0^2 - r^2 + (z_0 - z)^2}{a(\underline{\mathbf{x}};\underline{\mathbf{x}}_0) - b(r;r_0)}E(m(\underline{\mathbf{x}};\underline{\mathbf{x}}_0))\\
&\qquad - K(m(\underline{\mathbf{x}};\underline{\mathbf{x}}_0))]\\
&\quad + n_z(\underline{\mathbf{x}})\frac{z_0 - z}{a(\underline{\mathbf{x}};\underline{\mathbf{x}}_0) - b(r;r_0)}E(m(\underline{\mathbf{x}};\underline{\mathbf{x}}_0))\},
\end{aligned} \tag{14}$$

with H denoting the unit-step Heaviside function, the functions $m(\underline{\mathbf{x}};\underline{\mathbf{x}}_0)$, $a(\underline{\mathbf{x}};\underline{\mathbf{x}}_0)$, $K(m)$ and $E(m)$ given by

$$\begin{aligned}
m(\underline{\mathbf{x}};\underline{\mathbf{x}}_0) &= \frac{2b(r;r_0)}{a(\underline{\mathbf{x}};\underline{\mathbf{x}}_0)+b(r;r_0)},\\
a(\underline{\mathbf{x}};\underline{\mathbf{x}}_0) &= r_0^2+r^2+(z_0-z)^2,\\
b(r;r_0) &= 2rr_0,\\
K(m) &= \int_0^{\pi/2}\frac{d\theta}{\sqrt{1-m\sin^2\theta}},\\
E(m) &= \int_0^{\pi/2}\sqrt{1-m\sin^2\theta}d\theta,
\end{aligned} \tag{15}$$

the function $G_0^{(2)}(\underline{\mathbf{x}};\underline{\mathbf{x}}_0)$ being any solution of

$$\frac{\partial^2}{\partial r^2}[G_0^{(2)}(\underline{\mathbf{x}};\underline{\mathbf{x}}_0)]+\frac{1}{r}\frac{\partial}{\partial r}[G_0^{(2)}(\underline{\mathbf{x}};\underline{\mathbf{x}}_0)]+\frac{\partial^2}{\partial z^2}[G_0^{(2)}(\underline{\mathbf{x}};\underline{\mathbf{x}}_0)]=0 \quad \text{for } \underline{\mathbf{x}}\in\Omega_1\cup\Omega_2, \tag{16}$$

and the function $G_1^{(2)}(\underline{\mathbf{x}};\underline{\mathbf{x}}_0;\underline{\mathbf{n}}(\underline{\mathbf{x}}))$ defined by

$$G_1^{(2)}(\underline{\mathbf{x}};\underline{\mathbf{x}}_0;\underline{\mathbf{n}}(\underline{\mathbf{x}}))=n_r(\underline{\mathbf{x}})\frac{\partial}{\partial r}[G_0^{(2)}(\underline{\mathbf{x}};\underline{\mathbf{x}}_0)]+n_z(\underline{\mathbf{x}})\frac{\partial}{\partial z}[G_0^{(2)}(\underline{\mathbf{x}};\underline{\mathbf{x}}_0)]. \tag{17}$$

We may multiply κ_1 and κ_2 to (9) and (10) respectively and add up the two equations to obtain

$$\begin{aligned}
&\gamma_1(\underline{\mathbf{x}}_0)\kappa_1T(\underline{\mathbf{x}}_0)+\gamma_2(\underline{\mathbf{x}}_0)\kappa_2T(\underline{\mathbf{x}}_0)\\
&=\sum_{i=1}^{2}\int\limits_{\Gamma_i}\kappa_i(T(\underline{\mathbf{x}})G_1(\underline{\mathbf{x}};\underline{\mathbf{x}}_0;\underline{\mathbf{n}}(\underline{\mathbf{x}}))-G_0(\underline{\mathbf{x}};\underline{\mathbf{x}}_0)P(\underline{\mathbf{x}};\underline{\mathbf{n}}(\underline{\mathbf{x}})))rds(\underline{\mathbf{x}})\\
&+\int_a^b\kappa_1(T(r,0^-)G_1(r,0^-;\underline{\mathbf{x}}_0;0,1)-G_0(r,0^-;\underline{\mathbf{x}}_0)\,\frac{\partial}{\partial z}[T(\underline{\mathbf{x}})]\bigg|_{z=0^-})rdr\\
&-\int_a^b\kappa_2(T(r,0^+)G_1(r,0^+;\underline{\mathbf{x}}_0;0,1)-G_0(r,0^+;\underline{\mathbf{x}}_0)\,\frac{\partial}{\partial z}[T(\underline{\mathbf{x}})]\bigg|_{z=0^+})rdr\\
&\qquad\qquad\text{for } \underline{\mathbf{x}}_0\in\Omega_1\cup\Omega_2\cup\Gamma_1\cup\Gamma_2.
\end{aligned} \tag{18}$$

In general, we may take $G_0^{(2)}(\underline{\mathbf{x}};\underline{\mathbf{x}}_0)$ in (14) to be $G_0^{(2)}(\underline{\mathbf{x}};\underline{\mathbf{x}}_0) = 0$. Nevertheless, we may find it advantageous to solve (16) for $G_0^{(2)}(\underline{\mathbf{x}};\underline{\mathbf{x}}_0)$ that satisfies certain thermal conditions on the interface Γ_0 of the bimaterial. As we shall show below, a specially chosen $G_0^{(2)}(\underline{\mathbf{x}};\underline{\mathbf{x}}_0)$ may be used in (14) for the integral equation (18) such that the integrals over the interface Γ_0 vanishes.

3.2 Green's function for low conducting interface

For the case in which the interface Γ_0 of the bimaterial is low conducting, $G_0^{(2)}(\underline{\mathbf{x}};\underline{\mathbf{x}}_0)$ is chosen in such a way that $G_0(\underline{\mathbf{x}};\underline{\mathbf{x}}_0)$ in (14) satisfies the interfacial conditions

$$\left.\begin{array}{r} \kappa_2 \left.\dfrac{\partial G_0}{\partial z}\right|_{z=0^+} = \kappa_1 \left.\dfrac{\partial G_0}{\partial z}\right|_{z=0^-} \\ \lambda[G_0(r,0^+;\underline{\mathbf{x}}_0) - G_0(r,0^-;\underline{\mathbf{x}}_0))] = \kappa_2 \left.\dfrac{\partial G_0}{\partial z}\right|_{z=0^+} \end{array}\right\} \text{for } 0 < r < \infty. \quad (19)$$

The Green's function $G_0(\underline{\mathbf{x}};\underline{\mathbf{x}}_0)$ satisfying (19) can be obtained by performing an axial integration on the corresponding Green's function for three-dimensional heat conduction across a low conducting planar interface at $z = 0$. The analysis in Wang and Sudak [6] may be easily adapted to derive the corresponding three-dimensional Green's function. The derivation is given in the Appendix. If we let $x = r\cos\theta$, $y = r\sin\theta$, $\xi = r_0$, $\eta = 0$ and $\zeta = z_0$ in the three-dimensional Green's function for the low conducting interface and integrate it with respect to θ from $\theta = 0$ to $\theta = 2\pi$, we find that the required axisymmetric Green's function $G_0(\underline{\mathbf{x}};\underline{\mathbf{x}}_0)$ for low conducting Γ_0

is given by (14) with

$$
\begin{aligned}
& G_0^{(2)}(\underline{\mathbf{x}};\underline{\mathbf{x}}_0) \\
= \; & H(-z_0)\{H(-z)[G_0^{(1)}(\underline{\mathbf{x}};r_0,-z_0) \\
& -\frac{2\lambda}{\kappa_1}\int_0^\infty G_0^{(1)}(\underline{\mathbf{x}};r_0,u-z_0)\exp(-\frac{\lambda}{\kappa_2}(1+\frac{\kappa_2}{\kappa_1})u)du] \\
& +H(z)\frac{2\lambda}{\kappa_2}\int_0^\infty G_0^{(1)}(\underline{\mathbf{x}};r_0,z_0-u)\exp(-\frac{\lambda}{\kappa_2}(1+\frac{\kappa_2}{\kappa_1})u)du\} \\
& +H(z_0)\{H(z)[G_0^{(1)}(\underline{\mathbf{x}};r_0,-z_0) \\
& -\frac{2\lambda}{\kappa_2}\int_0^\infty G_0^{(1)}(\underline{\mathbf{x}};r_0,-z_0-u)\exp(-\frac{\lambda}{\kappa_2}(1+\frac{\kappa_2}{\kappa_1})u)du] \\
& +H(-z)\frac{2\lambda}{\kappa_1}\int_0^\infty G_0^{(1)}(\underline{\mathbf{x}};r_0,z_0+u)\exp(-\frac{\lambda}{\kappa_2}(1+\frac{\kappa_2}{\kappa_1})u)du\}.
\end{aligned}
\tag{20}
$$

Note that $G_0^{(2)}(\underline{\mathbf{x}};\underline{\mathbf{x}}_0)$ is obtained by integrating axially $\Phi^*(x,y,z;\xi,\eta,\zeta)$ given in the Appendix by (A4) and (A11).

The function $G_1^{(2)}(\underline{\mathbf{x}};\underline{\mathbf{x}}_0;\underline{\mathbf{n}}(\underline{\mathbf{x}}))$ which corresponds to $G_0^{(2)}(\underline{\mathbf{x}};\underline{\mathbf{x}}_0)$ in (20) is given by

$$
\begin{aligned}
& G_1^{(2)}(\underline{\mathbf{x}};\underline{\mathbf{x}}_0;\underline{\mathbf{n}}(\underline{\mathbf{x}})) \\
= \; & H(-z_0)\{H(-z)[G_1^{(1)}(\underline{\mathbf{x}};r_0,-z_0;\underline{\mathbf{n}}(\underline{\mathbf{x}})) \\
& -\frac{2\lambda}{\kappa_1}\int_0^\infty G_1^{(1)}(\underline{\mathbf{x}};r_0,u-z_0;\underline{\mathbf{n}}(\underline{\mathbf{x}}))\exp(-\frac{\lambda}{\kappa_2}(1+\frac{\kappa_2}{\kappa_1})u)du] \\
& +H(z)\frac{2\lambda}{\kappa_2}\int_0^\infty G_1^{(1)}(\underline{\mathbf{x}};r_0,z_0-u;\underline{\mathbf{n}}(\underline{\mathbf{x}}))\exp(-\frac{\lambda}{\kappa_2}(1+\frac{\kappa_2}{\kappa_1})u)du\} \\
& +H(z_0)\{H(z)[G_1^{(1)}(\underline{\mathbf{x}};r_0,-z_0;\underline{\mathbf{n}}(\underline{\mathbf{x}})) \\
& -\frac{2\lambda}{\kappa_2}\int_0^\infty G_1^{(1)}(\underline{\mathbf{x}};r_0,-z_0-u;\underline{\mathbf{n}}(\underline{\mathbf{x}}))\exp(-\frac{\lambda}{\kappa_2}(1+\frac{\kappa_2}{\kappa_1})u)du] \\
& +H(-z)\frac{2\lambda}{\kappa_1}\int_0^\infty G_1^{(1)}(\underline{\mathbf{x}};r_0,z_0+u;\underline{\mathbf{n}}(\underline{\mathbf{x}}))\exp(-\frac{\lambda}{\kappa_2}(1+\frac{\kappa_2}{\kappa_1})u)du\}.
\end{aligned}
\tag{21}
$$

Using (4) and (19) for low conducting Γ_0, we find that (18) can be reduced to

$$
\begin{aligned}
&\{\gamma_1(\underline{\mathbf{x}}_0)\kappa_1 + \gamma_2(\underline{\mathbf{x}}_0)\kappa_2\}T(\underline{\mathbf{x}}_0) \\
&= \sum_{i=1}^{2} \int\limits_{\Gamma_i} \kappa_i (T(\underline{\mathbf{x}}) G_1(\underline{\mathbf{x}}; \underline{\mathbf{x}}_0; \underline{\mathbf{n}}(\underline{\mathbf{x}})) - G_0(\underline{\mathbf{x}}; \underline{\mathbf{x}}_0) P(\underline{\mathbf{x}}; \underline{\mathbf{n}}(\underline{\mathbf{x}}))) r ds(\underline{\mathbf{x}}) \\
&\qquad\qquad \text{for } \underline{\mathbf{x}}_0 \in \Omega_1 \cup \Omega_2 \cup \Gamma_1 \cup \Gamma_2, \qquad (22)
\end{aligned}
$$

if $G_0(\underline{\mathbf{x}}; \underline{\mathbf{x}}_0)$ and $G_1(\underline{\mathbf{x}}; \underline{\mathbf{x}}_0; \underline{\mathbf{n}}(\underline{\mathbf{x}}))$ are given by (14) with (20) and (21).

If (22) is used to derive a boundary element procedure for the numerical solution of the problem stated in Section 2, it is not necessary to discretize the low conducting interface Γ_0 into boundary elements. Thus, the system of linear algebraic equations in the boundary element formulation is smaller with fewer unknowns.

3.3 Green's function for high conducting interface

For the case in which the interface Γ_0 of the bimaterial is high conducting, $G_0^{(2)}(\underline{\mathbf{x}}; \underline{\mathbf{x}}_0)$ is chosen in such a way that $G_0(\underline{\mathbf{x}}; \underline{\mathbf{x}}_0)$ in (14) satisfies the interfacial conditions

$$
\left.
\begin{aligned}
G_0(r, 0^+; \underline{\mathbf{x}}_0) = G_0(r, 0^-; \underline{\mathbf{x}}_0) \\
\kappa_2 \left.\frac{\partial G_0}{\partial z}\right|_{z=0^+} - \kappa_1 \left.\frac{\partial G_0}{\partial z}\right|_{z=0^-} = \alpha \left.\frac{\partial^2 G_0}{\partial z^2}\right|_{z=0}
\end{aligned}
\right\} \text{ for } 0 < r < \infty. \qquad (23)
$$

The function $G_0^{(2)}(\underline{\mathbf{x}}; \underline{\mathbf{x}}_0)$ such that (23) holds is obtained by integrating axially $\Phi^*(x, y, z; \xi, \eta, \zeta)$ given by (A4) and (A19) in the Appendix (for three-dimensional heat conduction across a high conducting planar interface at

$z=0$), that is,

$$
\begin{aligned}
& G_0^{(2)}(\underline{\mathbf{x}};\underline{\mathbf{x}}_0) \\
= \; & H(-z_0)\{H(-z)[-G_0^{(1)}(\underline{\mathbf{x}};r_0,-z_0) \\
& +\frac{2\kappa_1}{\alpha}\int_0^\infty G_0^{(1)}(\underline{\mathbf{x}};r_0,u-z_0)\exp(-\frac{1}{\alpha}(\kappa_1+\kappa_2)u)du] \\
& +H(z)\frac{2\kappa_1}{\alpha}\int_0^\infty G_0^{(1)}(\underline{\mathbf{x}};r_0,z_0-u)\exp(-\frac{1}{\alpha}(\kappa_1+\kappa_2)u)du\} \\
& +H(z_0)\{H(z)[-G_0^{(1)}(\underline{\mathbf{x}};r_0,-z_0) \\
& +\frac{2\kappa_2}{\alpha}\int_0^\infty G_0^{(1)}(\underline{\mathbf{x}};r_0,-z_0-u)\exp(-\frac{1}{\alpha}(\kappa_1+\kappa_2)u)du] \\
& +H(-z)\frac{2\kappa_2}{\alpha}\int_0^\infty G_0^{(1)}(\underline{\mathbf{x}};r_0,z_0+u)\exp(-\frac{1}{\alpha}(\kappa_1+\kappa_2)u)du\}.
\end{aligned} \tag{24}
$$

The function $G_1^{(2)}(\underline{\mathbf{x}};\underline{\mathbf{x}}_0;\underline{\mathbf{n}}(\underline{\mathbf{x}}))$ which corresponds to $G_0^{(2)}(\underline{\mathbf{x}};\underline{\mathbf{x}}_0)$ in (24) is given by

$$
\begin{aligned}
& G_1^{(2)}(\underline{\mathbf{x}};\underline{\mathbf{x}}_0;\underline{\mathbf{n}}(\underline{\mathbf{x}})) \\
= \; & H(-z_0)\{H(-z)[-G_1^{(1)}(\underline{\mathbf{x}};r_0,-z_0;\underline{\mathbf{n}}(\underline{\mathbf{x}})) \\
& +\frac{2\kappa_1}{\alpha}\int_0^\infty G_1^{(1)}(\underline{\mathbf{x}};r_0,u-z_0;\underline{\mathbf{n}}(\underline{\mathbf{x}}))\exp(-\frac{1}{\alpha}(\kappa_1+\kappa_2)u)du] \\
& +H(z)\frac{2\kappa_1}{\alpha}\int_0^\infty G_1^{(1)}(\underline{\mathbf{x}};r_0,z_0-u;\underline{\mathbf{n}}(\underline{\mathbf{x}}))\exp(-\frac{1}{\alpha}(\kappa_1+\kappa_2)u)du\} \\
& +H(z_0)\{H(z)[-G_1^{(1)}(\underline{\mathbf{x}};r_0,-z_0;\underline{\mathbf{n}}(\underline{\mathbf{x}})) \\
& +\frac{2\kappa_2}{\alpha}\int_0^\infty G_1^{(1)}(\underline{\mathbf{x}};r_0,-z_0-u;\underline{\mathbf{n}}(\underline{\mathbf{x}}))\exp(-\frac{1}{\alpha}(\kappa_1+\kappa_2)u)du] \\
& +H(-z)\frac{2\kappa_2}{\alpha}\int_0^\infty G_1^{(1)}(\underline{\mathbf{x}};r_0,z_0+u;\underline{\mathbf{n}}(\underline{\mathbf{x}}))\exp(-\frac{1}{\alpha}(\kappa_1+\kappa_2)u)du\}.
\end{aligned} \tag{25}
$$

For high conducting Γ_0, using (6), (7) and (23) and noting that

$$
\left.\frac{\partial^2 G_0}{\partial z^2}\right|_{z=0} = -\frac{1}{r}\frac{\partial}{\partial r}(r\frac{\partial}{\partial r}[G_0(r,0;\underline{\mathbf{x}}_0)]), \tag{26}
$$

we find that (18) can be rewritten as

$$\begin{aligned}
&\gamma_1(\underline{\mathbf{x}}_0)\kappa_1 T(\underline{\mathbf{x}}_0) + \gamma_2(\underline{\mathbf{x}}_0)\kappa_2 T(\underline{\mathbf{x}}_0) \\
&= \sum_{i=1}^{2} \int\limits_{\Gamma_i} \kappa_i (T(\underline{\mathbf{x}}) G_1(\underline{\mathbf{x}}; \underline{\mathbf{x}}_0; \underline{\mathbf{n}}(\underline{\mathbf{x}})) - G_0(\underline{\mathbf{x}}; \underline{\mathbf{x}}_0) P(\underline{\mathbf{x}}; \underline{\mathbf{n}}(\underline{\mathbf{x}}))) r ds(\underline{\mathbf{x}}) \\
&+ \int_a^b \alpha \{ -G_0(r, 0; \underline{\mathbf{x}}_0) \, \frac{1}{r} \frac{\partial}{\partial r} (r \frac{\partial T}{\partial r}) \bigg|_{z=0^+} + T(r, 0) \frac{1}{r} \frac{\partial}{\partial r} (r \frac{\partial}{\partial r} [G_0(r, 0; \underline{\mathbf{x}}_0)]) \} r dr \\
&\qquad\qquad\qquad \text{for } \underline{\mathbf{x}}_0 \in \Omega_1 \cup \Omega_2 \cup \Gamma_1 \cup \Gamma_2.
\end{aligned} \tag{27}$$

Using integration by parts, we find that

$$\begin{aligned}
& \int_a^b \alpha \{ -G_0(r, 0; \underline{\mathbf{x}}_0) \, \frac{1}{r} \frac{\partial}{\partial r} (r \frac{\partial T}{\partial r}) \bigg|_{z=0^+} \\
& + T(r, 0) \frac{1}{r} \frac{\partial}{\partial r} (r \frac{\partial}{\partial r} [G_0(r, 0; \underline{\mathbf{x}}_0)]) \} r dr \\
= \; & -b G_0(b, 0; \underline{\mathbf{x}}_0) \alpha \, \frac{\partial T}{\partial r} \bigg|_{(r,z)=(b,0)} + a G_0(a, 0; \underline{\mathbf{x}}_0) \alpha \, \frac{\partial T}{\partial r} \bigg|_{(r,z)=(a,0)} \\
& + b T(b, 0) \alpha \, \frac{\partial}{\partial r} [G_0(\underline{\mathbf{x}}; \underline{\mathbf{x}}_0)] \bigg|_{(r,z)=(b,0)} - a T(a, 0) \alpha \, \frac{\partial}{\partial r} [G_0(\underline{\mathbf{x}}; \underline{\mathbf{x}}_0)] \bigg|_{(r,z)=(a,0)} .
\end{aligned} \tag{28}$$

It follows that (27) reduces to

$$\begin{aligned}
& \{ \gamma_1(\underline{\mathbf{x}}_0)\kappa_1 + \gamma_2(\underline{\mathbf{x}}_0)\kappa_2 \} T(\underline{\mathbf{x}}_0) \\
& - b T(b, 0) \alpha \, \frac{\partial}{\partial r} [G_0(\underline{\mathbf{x}}; \underline{\mathbf{x}}_0)] \bigg|_{(r,z)=(b,0)} + a T(a, 0) \alpha \, \frac{\partial}{\partial r} [G_0(\underline{\mathbf{x}}; \underline{\mathbf{x}}_0)] \bigg|_{(r,z)=(a,0)} \\
& + b G_0(b, 0; \underline{\mathbf{x}}_0) \alpha \, \frac{\partial T}{\partial r} \bigg|_{(r,z)=(b,0)} - a G_0(a, 0; \underline{\mathbf{x}}_0) \alpha \, \frac{\partial T}{\partial r} \bigg|_{(r,z)=(a,0)} \\
& = \sum_{i=1}^{2} \int\limits_{\Gamma_i} \kappa_i (T(\underline{\mathbf{x}}) G_1(\underline{\mathbf{x}}; \underline{\mathbf{x}}_0; \underline{\mathbf{n}}(\underline{\mathbf{x}})) - G_0(\underline{\mathbf{x}}; \underline{\mathbf{x}}_0) P(\underline{\mathbf{x}}; \underline{\mathbf{n}}(\underline{\mathbf{x}}))) r ds(\underline{\mathbf{x}}) \\
& \qquad\qquad\qquad \text{for } \underline{\mathbf{x}}_0 \in \Omega_1 \cup \Omega_2 \cup \Gamma_1 \cup \Gamma_2.
\end{aligned} \tag{29}$$

Thus, the integral over the high conducting interface Γ_0 vanishes if the Green's function $G_0(\underline{\mathbf{x}}; \underline{\mathbf{x}}_0)$ is given by (14) with $G_0^{(2)}(\underline{\mathbf{x}}; \underline{\mathbf{x}}_0)$ in (25).

3.4 Boundary element procedures

In this section, we describe boundary element procedures for determining $T(\underline{\mathbf{x}})$ and $P(\underline{\mathbf{x}};\underline{\mathbf{n}}(\underline{\mathbf{x}}))$ (whichever is not known) on $\Gamma_1 \cup \Gamma_2$. Once $T(\underline{\mathbf{x}})$ and $P(\underline{\mathbf{x}};\underline{\mathbf{n}}(\underline{\mathbf{x}}))$ are completely known on $\Gamma_1 \cup \Gamma_2$, we can obtain the temperature at any point $\underline{\mathbf{x}}_0$ in the interior of the domains by using $\gamma_1(\underline{\mathbf{x}}_0) = 1$ and $\gamma_2(\underline{\mathbf{x}}_0) = 0$ for $\underline{\mathbf{x}}_0$ in the interior of Ω_1 or $\gamma_1(\underline{\mathbf{x}}_0) = 0$ and $\gamma_2(\underline{\mathbf{x}}_0) = 1$ for $\underline{\mathbf{x}}_0$ in the interior of Ω_2 in (22) (for low conducting interface) or in (29) (for high conducting interface).

We discretize the boundary $\Gamma_1 \cup \Gamma_2$ into N straight line elements denoted by $B^{(1)}$, $B^{(2)}$, $\cdots$, $B^{(N-1)}$ and $B^{(N)}$. As (22) or (29) does not contain any integral over the low conducting interface (because of the use of the special Green's function), we do not need to discretize the interface Γ_0.

For a simple approximation, T and P are taken to be constants over an element of $\Gamma_1 \cup \Gamma_2$, specifically

$$\left.\begin{array}{r} T(\underline{\mathbf{x}}) \simeq T^{(m)} \\ P(\underline{\mathbf{x}};\underline{\mathbf{n}}(\underline{\mathbf{x}})) \simeq P^{(m)} \end{array}\right\} \text{ for } \underline{\mathbf{x}} \in B^{(m)} \ (m = 1, 2, \cdots , N), \tag{30}$$

where $T^{(m)}$ and $P^{(m)}$ are constants.

Each boundary element is associated with only one unknown constant. Specifically, if T is specified over the element $B^{(m)}$ according to the first line of (8) then $P^{(m)}$ is the unknown over $B^{(m)}$. On the other hand, if P is given by the second line of (8) over $B^{(m)}$, we can express $P^{(m)}$ in terms of $T^{(m)}$ and regard $T^{(m)}$ as the unknown constant over $B^{(m)}$.

3.4.1 Low conducting interface

For low conducting interface Γ_0, letting $\underline{\mathbf{x}}_0$ in (22) be given in turn by the midpoints of $B^{(i)}$ $(i = 1, 2, \cdots, N)$, together with (8), we obtain

$$
\begin{aligned}
&\{\gamma_1(\widehat{\underline{\mathbf{x}}}^{(i)})\kappa_1 + \gamma_2(\widehat{\underline{\mathbf{x}}}^{(i)})\kappa_2\}[d^{(i)}T^{(i)} + (1 - d^{(i)})f_0(\widehat{\underline{\mathbf{x}}}^{(i)})] \\
&= \sum_{m=1}^{N} \kappa^{(m)}\{[d^{(m)}T^{(m)} + (1 - d^{(m)})f_0(\widehat{\underline{\mathbf{x}}}^{(m)})] \int\limits_{B^{(m)}} G_1(\underline{\mathbf{x}}; \widehat{\underline{\mathbf{x}}}^{(i)}; \underline{\mathbf{n}}^{(m)}) r ds(\underline{\mathbf{x}}) \\
&- [d^{(m)}(f_1(\widehat{\underline{\mathbf{x}}}^{(m)}) + f_2(\widehat{\underline{\mathbf{x}}}^{(m)})T^{(m)}) + (1 - d^{(m)})P^{(m)}] \int\limits_{B^{(m)}} G_0(\underline{\mathbf{x}}; \widehat{\underline{\mathbf{x}}}^{(i)}) r ds(\underline{\mathbf{x}})\} \\
&\qquad\qquad\qquad\qquad \text{for } i = 1,\ 2, \cdots, N, \qquad (31)
\end{aligned}
$$

where $\widehat{\underline{\mathbf{x}}}^{(i)}$ is the midpoint of $B^{(i)}$, $d^{(m)} = 0$ if T is specified on the m-th element $B^{(m)}$ as given by the first line of (8), $d^{(m)} = 1$ if the boundary condition given by the second line of (8) is applicable on $B^{(m)}$, $\underline{\mathbf{n}}^{(m)}$ is the unit normal vector to $B^{(m)}$ pointing away from the solution domain $\Omega_1 \cup \Omega_2$, $\kappa^{(m)} = \kappa_1$ if $B^{(m)}$ is an element on the boundary of Ω_1 and $\kappa^{(m)} = \kappa_2$ if $B^{(m)}$ is an element on the boundary of Ω_2.

In (31), the integrals over $B^{(m)}$ are Cauchy principal if $\widehat{\underline{\mathbf{x}}}^{(i)}$ is the midpoint of $B^{(m)}$ (that is, if $m = i$). The Cauchy principal integrals can be accurately evaluated by using a highly accurate Gaussian quadrature.

Now (31) gives a system of N linear algebraic equations containing N unknowns given by either $T^{(k)}$ or $P^{(k)}$ $(k = 1, 2, \cdots, N)$. Once the unknowns on the boundary are determined, the temperature at the interior point of the domain $\Omega_1 \cup \Omega_2$ can be obtained as explained above.

3.4.2 High conducting interface

For high conducting interface Γ_0, if we proceed as before by collocating (29) at the midpoint of each boundary element, we obtain

$$
\begin{aligned}
& \{\gamma_1(\underline{\widehat{\mathbf{x}}}^{(i)})\kappa_1 + \gamma_2(\underline{\widehat{\mathbf{x}}}^{(i)})\kappa_2\}[d^{(i)}T^{(i)} + (1-d^{(i)})f_0(\underline{\widehat{\mathbf{x}}}^{(i)})] \\
& -bT(b,0)\alpha \left.\frac{\partial}{\partial r}[G_0(\underline{\mathbf{x}};\underline{\mathbf{x}}_0)]\right|_{(r,z)=(b,0)} + aT(a,0)\alpha \left.\frac{\partial}{\partial r}[G_0(\underline{\mathbf{x}};\underline{\mathbf{x}}_0)]\right|_{(r,z)=(a,0)} \\
& +bG_0(b,0;\underline{\mathbf{x}}_0)\alpha \left.\frac{\partial T}{\partial r}\right|_{(r,z)=(b,0)} - aG_0(a,0;\underline{\mathbf{x}}_0)\alpha \left.\frac{\partial T}{\partial r}\right|_{(r,z)=(a,0)} \\
= & \sum_{m=1}^{N} \kappa^{(m)}\{[d^{(m)}T^{(m)} + (1-d^{(m)})f_0(\underline{\widehat{\mathbf{x}}}^{(m)})] \int\limits_{B^{(m)}} G_1(\underline{\mathbf{x}};\underline{\widehat{\mathbf{x}}}^{(i)};\underline{\mathbf{n}}^{(m)})rds(\underline{\mathbf{x}}) \\
& -[d^{(m)}(f_1(\underline{\widehat{\mathbf{x}}}^{(m)}) + f_2(\underline{\widehat{\mathbf{x}}}^{(m)})T^{(m)}) + (1-d^{(m)})P^{(m)}] \\
& \times \int\limits_{B^{(m)}} G_0(\underline{\mathbf{x}};\underline{\widehat{\mathbf{x}}}^{(i)})rds(\underline{\mathbf{x}})\} \\
& \qquad\qquad\qquad\qquad\qquad\qquad \text{for } i = 1,\ 2,\cdots,N, \qquad (32)
\end{aligned}
$$

where $\kappa^{(m)}$ is as defined below (31).

The terms $T(a,0)$, $T(b,0)$, $\left.\frac{\partial T}{\partial r}\right|_{(r,z)=(a,0)}$ and $\left.\frac{\partial T}{\partial r}\right|_{(r,z)=(b,0)}$ in (32) are unknown constants. They can, however, be approximated in terms of T and P on boundary elements near $(a,0)$ and/or $(b,0)$. How the required approximations may be made depends on the geometries of the solution domains − see, for example, Problems 3 and 4 in Section 4 below. Thus, (32) can be solved as a system of N linear algebraic equations for N unknowns given by either $T^{(k)}$ or $P^{(k)}$ $(k = 1, 2, ..., N)$.

4 Specific problems

Problem 1. To test the boundary element procedure for Γ_0 that is low conducting, consider the regions Ω_1 and Ω_2 as sketched in Figure 3. Note that Ω_1 and Ω_2 are defined by the curves $r^2 + z^2 = 4$ and $r^2 + z^2 = 1$ and the lines $r = 0$, $r = 1$, $r = 2$ and $z = -1$ on the rz plane. For a particular problem take $\kappa_1 = 1$, $\kappa_2 = 2$ and $\lambda = 1$. The exterior boundary of $\Omega_1 \cup \Omega_2$ is approximated using N straight line elements.

The boundary conditions on the exterior boundary of $\Omega_1 \cup \Omega_2$ are given by

$$\left.\begin{array}{rcr} P(2, z; 1, 0) & = & 4z \\ P(1, z; -1, 0) & = & -2z \end{array}\right\} \text{ for } -1 < z < 0,$$

$$\begin{aligned} T(r, -1) &= -r^2 + \frac{2}{3} \text{ for } 1 < r < 2, \\ T(r, z) &= \frac{1}{2}r^2 z - \frac{1}{3}z^3 + r^2 - 2z^2 \\ &\quad \text{for } r^2 + z^2 = 1,\ 0 < r < 1, \\ P(r, z; \frac{1}{2}r, \frac{1}{2}z) &= -\frac{1}{2}z^3 - 2z^2 + \frac{3}{4}r^2 z + r^2 \\ &\quad \text{for } r^2 + z^2 = 4,\ 0 < r < 2. \end{aligned}$$

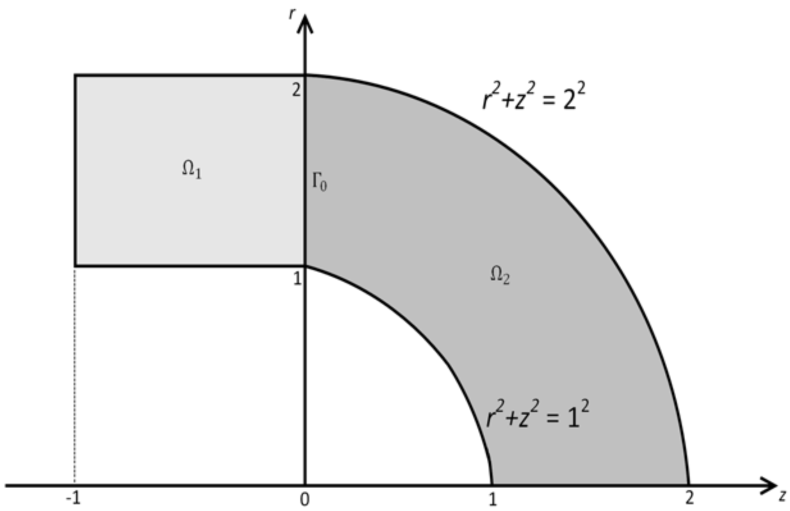

Figure 3. A geometrical sketch of Problem 1 on the rz plane.

It can be easily verified that the exact solution for the problem here is given by

$$T(r,z)=\begin{cases} r^2z-\frac{2}{3}z^3 & \text{for} \quad (r,z)\in\Omega_1, \\ \frac{1}{2}r^2z-\frac{1}{3}z^3+r^2-2z^2 & \text{for} \quad (r,z)\in\Omega_2. \end{cases}$$

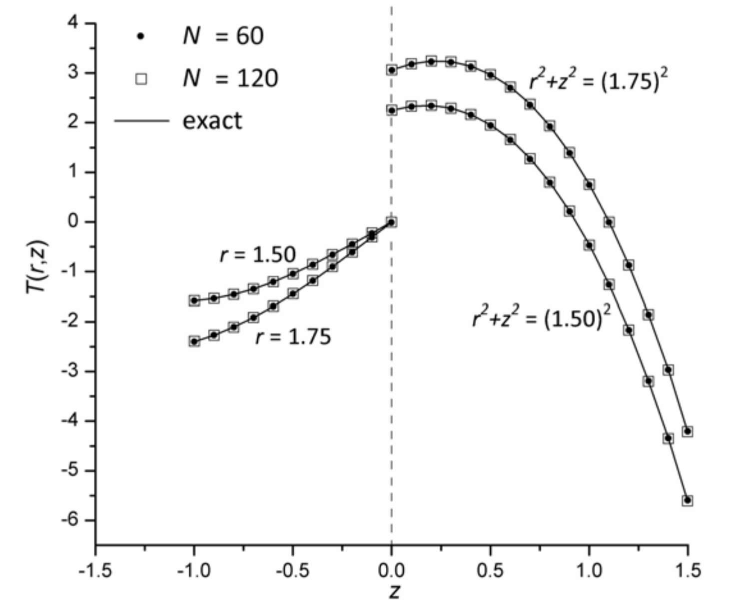

Figure 4. Plots of the numerical and exact temperature $T(r,z)$ for $-1 < z < 1.5$ (Problem 1).

Numerical values are obtained for the temperature at the interior of the regions by solving equation (31) using $N = 60$ and $N = 120$. Through the use of (22) with $\gamma_1(\underline{\mathbf{x}}_0) = 1, \gamma_2(\underline{\mathbf{x}}_0) = 0$ for $\underline{\mathbf{x}}_0$ in the interior of Ω_1 and

$\gamma_1(\underline{\mathbf{x}}_0) = 0, \gamma_2(\underline{\mathbf{x}}_0) = 1$ for $\underline{\mathbf{x}}_0$ in the interior of Ω_2, numerical values of the temperature at $r = 1.5$ and $r = 1.75$ for $-1 < z < 0$ and at $r^2 + z^2 = (1.75)^2$ and $r^2 + z^2 = (1.5)^2$ for $0 < z < 1.5$ are obtained and compared graphically with the exact temperature in Figure 4. On the whole, the numerical and exact temperature agree well with each other. Note that the gap in the graph is due to the temperature jump across the interface Γ_0 at $z = 0$.

Problem 2. Consider now the case in which Ω_1 and Ω_2 are given by

$$\begin{aligned} \Omega_1 &= \{(r,z):\ 0 \le r < 1,\ \ -1 < z < 0\}, \\ \Omega_2 &= \{(r,z):\ 0 \le r < \frac{3}{2},\ 0 < z < \frac{3}{2}\}, \end{aligned}$$

as sketched in Figure 5. As in Problem 1, the interface Γ_0 between Ω_1 and Ω_2 is taken to be low conducting. Note that for this particular case the exterior boundary of the bimaterial lies on part of the $z = 0$ plane (that is, $1 < r < 3/2$, $z = 0$).

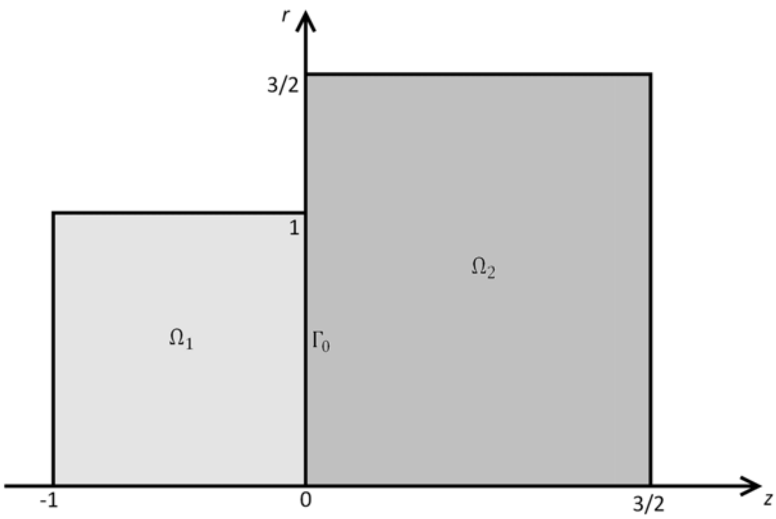

Figure 5. A geometrical sketch of Problem 2 on the rz plane.

For a particular problem, we take $\kappa_1 = 1$, $\kappa_2 = 1/2$ and $\lambda = 1$ and the boundary conditions as

$$
\begin{aligned}
T(1,z) &= 4 - 2z^2 + 2z \text{ for } -1 < z < 0, \\
P(r,-1;0,-1) &= -6 \text{ for } 0 < r < 1, \\
T(r,\frac{3}{2}) &= r^2 + \frac{13}{2} \text{ for } 0 < r < \frac{3}{2}, \\
P(\frac{3}{2},z;1,0) &= 3 \text{ for } 0 < z < \frac{3}{2}, \\
T(r,0) &= r^2 + 5 \text{ for } 1 < r < \frac{3}{2}.
\end{aligned}
$$

The exact solution for the particular problem here is given by

$$
T(r,z) = \begin{cases} r^2 - 2z^2 + 2z + 3 & \text{for} \quad (r,z) \in \Omega_1, \\ r^2 - 2z^2 + 4z + 5 & \text{for} \quad (r,z) \in \Omega_2. \end{cases}
$$

Table 1. Numerical and exact values of T at selected interior points for Problem 2.

Point	$N = 25$	$N = 50$	$N = 100$	$N = 200$	Exact
$(0.30, -0.80)$	0.21635	0.21094	0.21005	0.20996	0.21000
$(0.75, -0.35)$	2.61420	2.61655	2.61724	2.61743	2.61750
$(0.40, -0.40)$	2.03921	2.03947	2.03977	2.03992	2.04000
$(1.40, 0.20)$	7.60894	7.66118	7.67354	7.67800	7.68000
$(0.50, 1.25)$	7.11813	7.12282	7.12431	7.12478	7.12500
$(0.20, 0.80)$	6.94401	6.95498	6.95848	6.95954	6.96000

The exterior boundary of the bimaterial is discretized into N straight line elements. The numerical values of T at various selected points in $\Omega_1 \cup \Omega_2$ are computed using (22) with $\gamma_1(\underline{\mathbf{x}}_0) = 1$ and $\gamma_2(\underline{\mathbf{x}}_0) = 0$ for $\underline{\mathbf{x}}_0$ in the interior of Ω_1 and $\gamma_1(\underline{\mathbf{x}}_0) = 0$ and $\gamma_2(\underline{\mathbf{x}}_0) = 1$ for $\underline{\mathbf{x}}_0$ in the interior of Ω_2. They are compared with the exact values in Table 1 for $N = 25$, 50, 100 and 200. The numerical values are reasonably accurate and they converge to the exact solution when the calculation is refined by reducing the sizes of the boundary elements used (that is, when N is increased from 25 to 200). All percentage errors of the numerical values for $N = 200$ are less than 0.05%.

Problem 3. To check the boundary element procedure for a bimaterial with a high conducting interface, take

$$\begin{aligned}\Omega_1 &= \{(r,z):\ 0 \le r < 1,\ \ -1 < z < 0\},\\ \Omega_2 &= \{(r,z):\ 0 \le r < 1,\ 0 < z < 1\}.\end{aligned}$$

as illustrated in Figure 6.

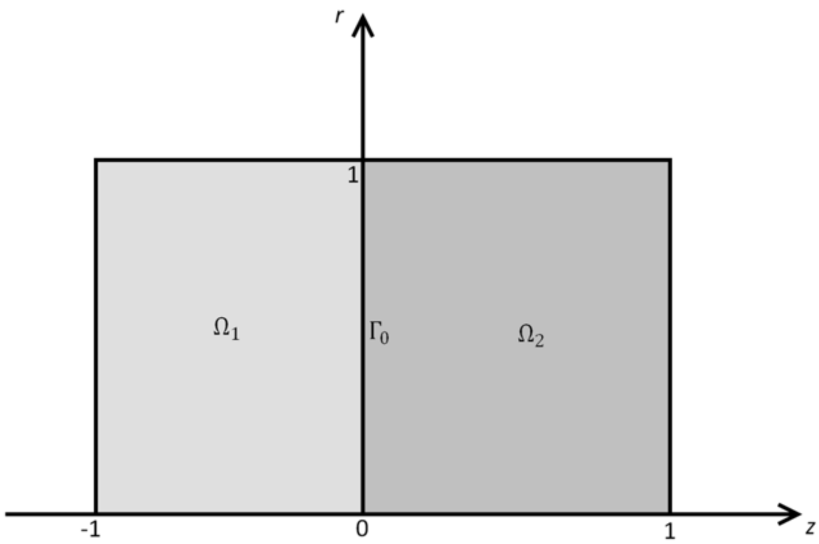

Figure 6. A geometrical sketch of Problem 3 on the rz plane.

We take $\kappa_1 = 6$, $\kappa_2 = 2$, and $\alpha = 7/4$ and the boundary conditions as

$$\begin{aligned} P(1,z;1,0) &= 4 + z \text{ for } -1 < z < 0, \\ T(1,z) &= 2 + \frac{1}{2}z - 4z^2 - z^3 \text{ for } 0 < z < 1, \end{aligned}$$

$$\left.\begin{aligned} T(r,-1) &= \tfrac{3}{2}r^2 - \tfrac{17}{3} \\ P(r,1;0,1) &= \tfrac{3}{2}r^2 - 12 \end{aligned}\right\} \text{for } 0 < r < 1.$$

The exact solution of the particular problem here is given by

$$T(r,z) = \begin{cases} 2r^2 - 4z^2 + \frac{1}{2}r^2 z - \frac{1}{3}z^3 + 2z & \text{for } (r,z) \in \Omega_1, \\ 2r^2 - 4z^2 + \frac{3}{2}r^2 z - z^3 - z & \text{for } (r,z) \in \Omega_2. \end{cases}$$

The exterior boundary of the bimaterial is discretized into N straight line elements. To solve (32) as a system of N linear algebraic equations in N unknowns, we have to approximate $T(1,0)$ and $\left.\dfrac{\partial T}{\partial r}\right|_{(r,z)=(1,0)}$ in terms of T and P on the boundary elements. (Note that for this particular problem, $a = 0$ and $b = 1$.) If the exterior boundary is discretized in such a way that the first and the last elements ($B^{(1)}$ and $B^{(N)}$ respectively) are of equal length, lie on $r = 1$ and have $(1,0)$ as one of their endpoints, then we can make the approximations

$$\begin{aligned} T(1,0) &\simeq \frac{1}{2}(T^{(1)} + T^{(N)}), \\ \left.\frac{\partial T}{\partial r}\right|_{(r,z)=(1,0)} &\simeq \frac{1}{2}(P^{(1)} + P^{(N)}). \end{aligned}$$

Numerical values of the temperature at selected interior points are compared with the exact values in Table 2. On the whole, the numerical values at the selected interior points are in good agreement with the exact solution and improve in accuracy when N is increased from 40 to 320 (again, calculation is refined by reducing the sizes of the boundary elements used). The numerical results here also justify the above approximations for the terms $T(1,0)$ and $\left.\dfrac{\partial T}{\partial r}\right|_{(r,z)=(1,0)}$ in (32).

Table 2. Numerical and exact values of T at selected interior points for Problem 3.

Point	$N = 40$	$N = 80$	$N = 160$	$N = 320$	Exact
$(0.500, -0.500)$	-1.52954	-1.52386	-1.52198	-1.52130	-1.52083
$(0.200, -0.100)$	-0.17288	-0.16598	-0.16350	-0.16249	-0.16167
$(0.700, -0.950)$	-4.47882	-4.47771	-4.47724	-4.47707	-4.47696
$(0.900, 0.900)$	-2.14050	-2.15158	-2.15451	-2.15525	-2.15550
$(0.100, 0.500)$	-1.59994	-1.59895	-1.59828	-1.59790	-1.59750
$(0.750, 0.001)$	1.10860	1.11827	1.12191	1.12347	1.12484

Problem 4. Problem 3 deals with relatively simple rectangular domains on the rz-plane. For a more general test problem involving a high conducting interface, we take here Ω_1 with a slanted boundary $r = z + 3/2$ and Ω_2 with part of $z = 0$ as its exterior boundary. A sketch of $\Omega_1 \cup \Omega_2$ is given in Figure 7.

We take $\kappa_1 = 1$, $\kappa_2 = 1/2$ and $\alpha = 1/8$ and the boundary conditions on the exterior boundary of $\Omega_1 \cup \Omega_2$ as

$$\begin{aligned} T(r, z) &= r^2 - 2z^2 + \frac{1}{2}r^2 z - \frac{1}{3}z^3 \\ \text{for } r &= z + \frac{3}{2}, -1 < z < 0, \\ P(r, -1; 0, -1) &= -3 - \frac{1}{2}r^2 \text{ for } 0 < r < \frac{1}{2}, \end{aligned}$$

$$\begin{aligned} P(r, 2; 0, 1) &= -17 + r^2 \text{ for } 0 < r < 2, \\ P(2, z; 1, 0) &= 4(1 + z) \text{ for } 0 < z < 2, \\ T(r, 0) &= r^2 \text{ for } \frac{3}{2} < r < 2. \end{aligned}$$

The exact solution of the problem here is given by

$$T(r, z) = \begin{cases} r^2 - 2z^2 + \frac{1}{2}r^2 z - \frac{1}{3}z^3 & \text{for } (r, z) \in \Omega_1, \\ r^2 - 2z^2 + r^2 z - \frac{2}{3}z^3 - z & \text{for } (r, z) \in \Omega_2. \end{cases}$$

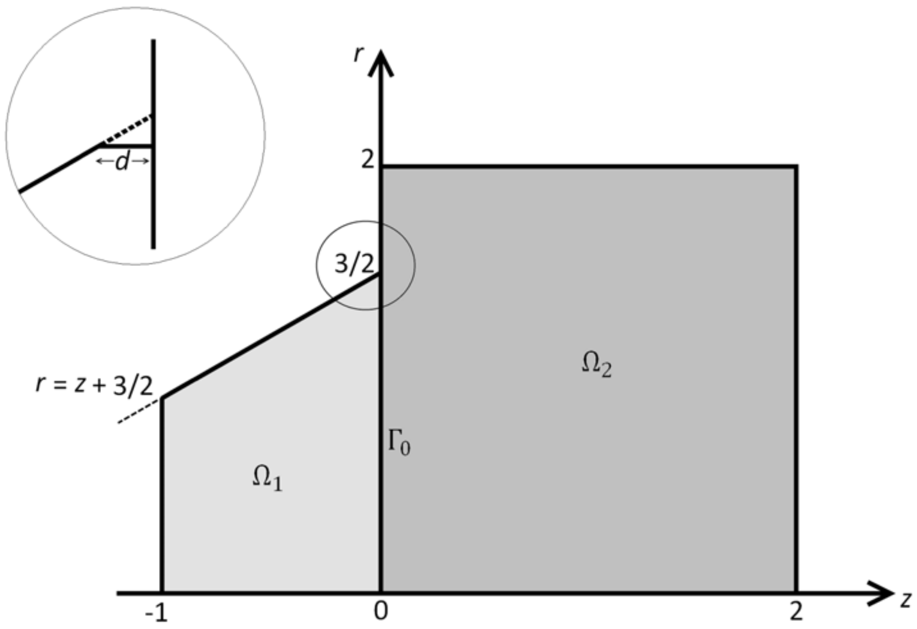

Figure 7. A geometrical sketch of Problem 4 on the rz plane.

To solve (32), we have to approximate $T(3/2,0)$ and $\left.\dfrac{\partial T}{\partial r}\right|_{(r,z)=(3/2,0)}$ in terms of T and P on the boundary elements which approximate the exterior boundary of $\Omega_1 \cup \Omega_2$. If there is a small horizontal boundary element at the intersection between the slanted boundary $r = z + 3/2$ and the vertical boundary $z = 0$ then $\left.\dfrac{\partial T}{\partial r}\right|_{(r,z)=(3/2,0)}$ can be approximated as P on that horizontal element. For this purpose, we approximate the line segment $r = z + 3/2$, $-d < z < 0$, where d is a very small number, by using a small horizontal line element of length d (see Figure 7). If the small horizontal line element is taken to be the first element $B^{(1)}$ then

$$\begin{aligned} T(3/2,0) &\simeq T^{(1)}, \\ \left.\frac{\partial T}{\partial r}\right|_{(r,z)=(3/2,0)} &\simeq P^{(1)}, \end{aligned}$$

where $T^{(1)}$ can be easily worked out from the given boundary conditions (since T is specified on $r = z+3/2$) and $P^{(1)}$ is an unknown to be determined.

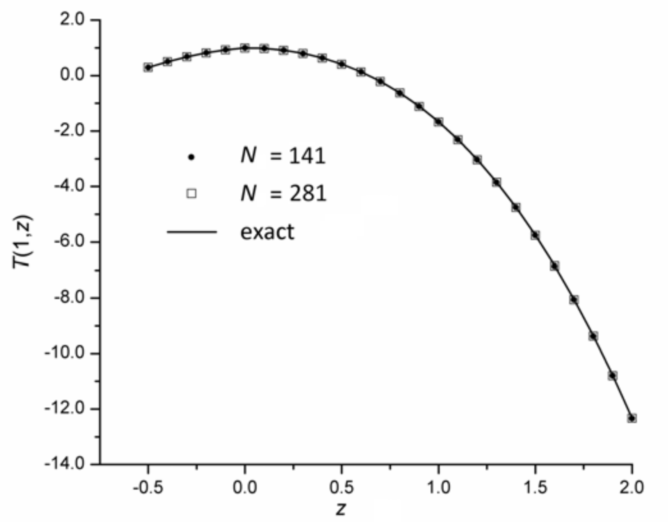

Figure 8. Plots of the numerical and exact boundary temperature $T(1, z)$ for $-\frac{1}{2} < z < 2$ (Problem 4).

Numerical values are obtained for T by using $N = 141$ and $N = 281$ with $d = 0.0001$.The numerical results are compared graphically with the exact solution as shown in Figure 8 and Figure 9. Figure 8 shows the temperature along $r = 1$ $(-\frac{1}{2} < z < 2)$ while Figure 9 captures the variation of the temperature at $z = 1$ and $z = 2$ $(0 < r < 2)$. On the whole, the numerical and exact temperature values agree well with each other.

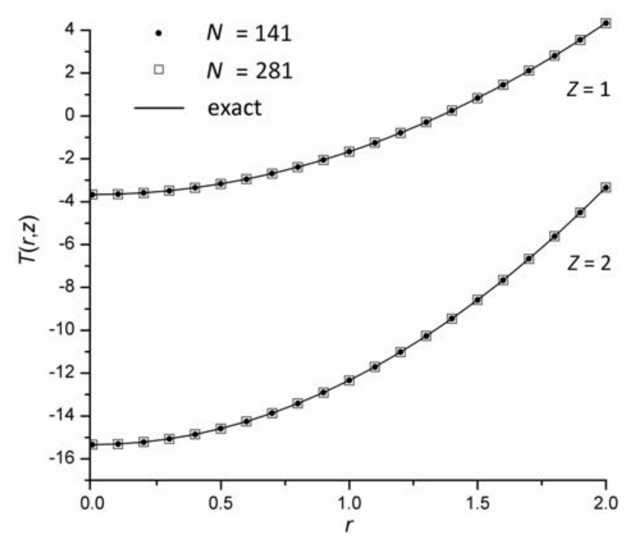

Figure 9. Plots of the numerical and exact boundary temperature $T(r, z)$ for $z = 1$ and $z = 2$ $(0 < r < 2)$ (Problem 4).

Problem 5. Here we consider a thermal management system modeled by two homogeneous cylindrical solids as sketched in Figure 10. The regions Ω_1 and Ω_2 model the computer chip and the heat sink respectively while the interface Γ_0 (line $z = 0$, $0 < r < r_2$) represents a thin layer of carbon nanotubes or nanocylinders of high thermal conductivity. We model the interface Γ_0 as high conducting.

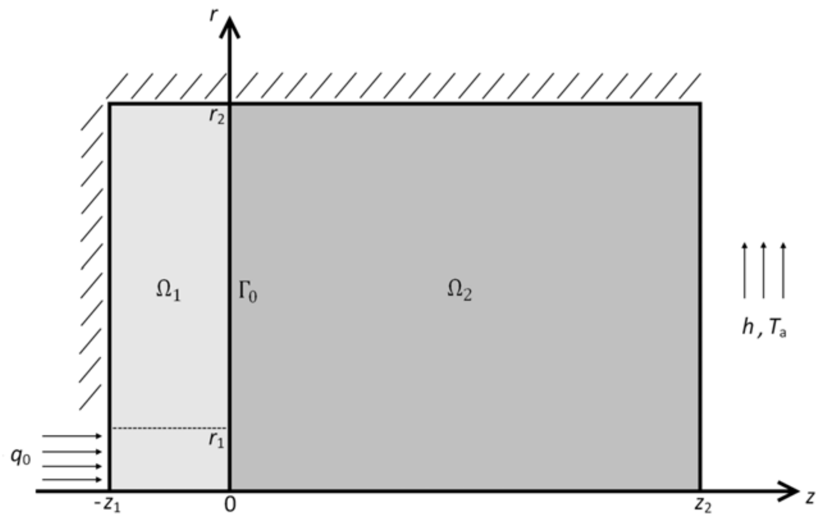

Figure 10. A geometrical sketch of Problem 5 on the rz plane.

A constant heat flux q_0 flows into the system through $z = -z_1$, $0 < r < r_1$. There is a uniform convective cooling at the end $z = z_2$, $0 < r < r_2$. Elsewhere, the exterior boundary of the thermal system is thermally insulated. More precisely, the boundary conditions on the sides that are not thermally insulated are as follows:

$$\begin{aligned} -\kappa_1 P(r, -z_1; 0, -1) &= q_0 \text{ for } 0 < r < r_1, \\ -\kappa_2 P(r, z_2; 0, 1) &= h[T(r, z_2) - T_{\mathrm{a}}] \text{ for } 0 < r < r_2, \end{aligned}$$

where q_0 is the magnitude of the specified heat flux , h is the heat convection coefficient and T_{a} is the ambient temperature of the system.

We study the effect of the interfacial parameter α (assumed to be constant) on the thermal performance of the heat dissipation system. For this purpose, we take the radii r_1 and r_2 and the lengths z_1 and z_2 to be $r_2/r_1 = 5$ and $z_2/z_1 = 5$. The numerical results are obtained by employing a total of

160 elements on the exterior boundary of $\Omega_1 \cup \Omega_2$. To capture the thermal behaviors more accurately near the region of heating, it may be necessary to employ more elements on the side $z = -z_1$, especially near the point $(r, z) = (r_1, -z_1)$ where the boundary heat flux is discontinuous. Using $hz_1/\kappa_1 = 2.5 \times 10^{-3}$ and $\kappa_2/\kappa_1 = 2.20$, the non-dimensionalized temperature $\kappa_1(T - T_{\mathrm{a}})/(q_0 z_1)$ along the z-axis are plotted against z/z_1 for selected values of the non-dimensionalized parameter $\alpha/(\kappa_1 z_1)$.

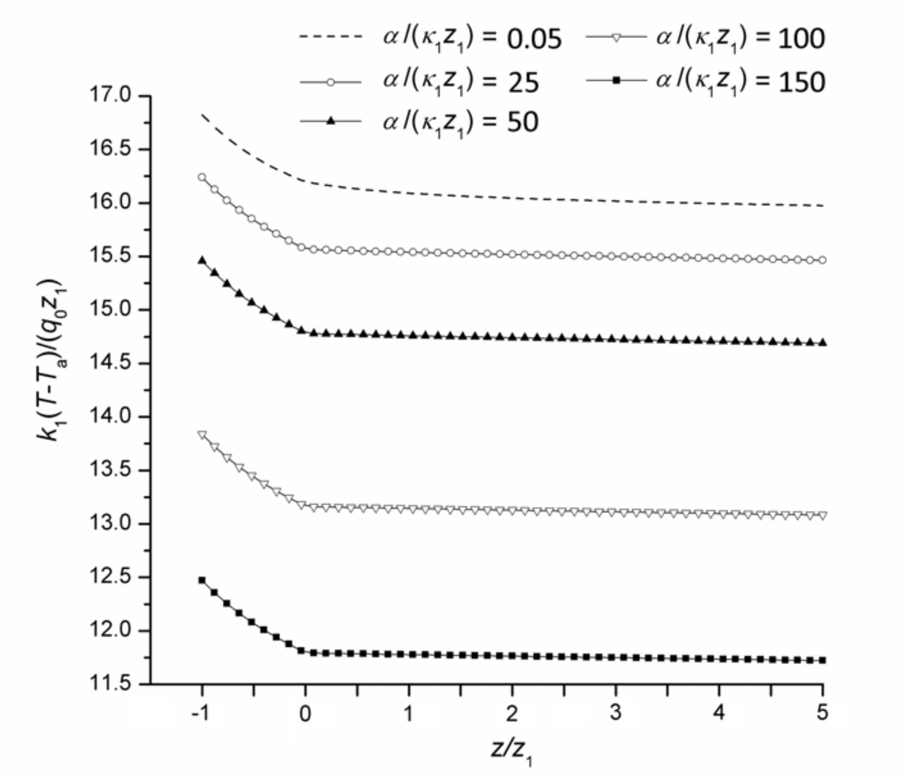

Figure 11. Plots of $\kappa_1(T - T_{\mathrm{a}})/(q_0 z_1)$ against z/z_1 for a few selected values of $\alpha/(\kappa_1 z_1)$ (for high conducting interfaces).

In Figure 11, the dashed line ($\alpha/(\kappa_1 z_1) = 0.05$) approximates the plot of the non-dimensionalized temperature profile for the case in which the interface between the chip and heat sink is nearly perfectly bonded (for perfectly bonded or ideal interface, $\alpha/(\kappa_1 z_1) = 0$). As anticipated, at a given point on the z-axis, the non-dimensionalized temperature in both the computer chip and heat sink decreases as $\alpha/(\kappa_1 z_1)$ increases. Hence, the thin layer of carbon nanotubes or nanocylinders of high thermal conductivity enhances the heat dissipation performance of the system.

Still with $r_2/r_1 = 5$, $z_2/z_1 = 5$, $hz_1/\kappa_1 = 2.5 \times 10^{-3}$ and $\kappa_2/\kappa_1 = 2.20$, we will now investigate the case whereby the interface between the chip and the sink is filled with microscopic voids. We regard this interface as low conducting. Again, we plot $\kappa_1(T - T_{\mathrm{a}})/(q_0 z_1)$ against $z/z_1$for selected values of the non-dimensionalized parameter $\lambda z_1/\kappa_1$ as shown in Figure 12. The dashed line ($\lambda z_1/\kappa_1 = 100$) gives the temperature profile for the case of a nearly ideal interface as there is negligible temperature jump across the interface at $z = 0$. Note that the dashed lines in both Figure 11 and Figure 12 give the temperature profile for a nearly perfect interface. The temperature in the chip in Figure 12 is higher than that in Figure 11. Thus, the effect of the low conducting interface on heat flow is opposite to that of the high conducting one, that is, the low conducting interface obstructs rather than enhance the heat flow from the chip into the sink. As expected, when the obstruction of the heat flow is higher (that is, when $\lambda z_1/\kappa_1$ has a lower value), the temperature jump across the interface at $z/z_1 = 0$ is bigger. Also, the differences between the temperature distributions for the different values of $\lambda z_1/\kappa_1$ are much smaller in the sink compared to those in the chip.

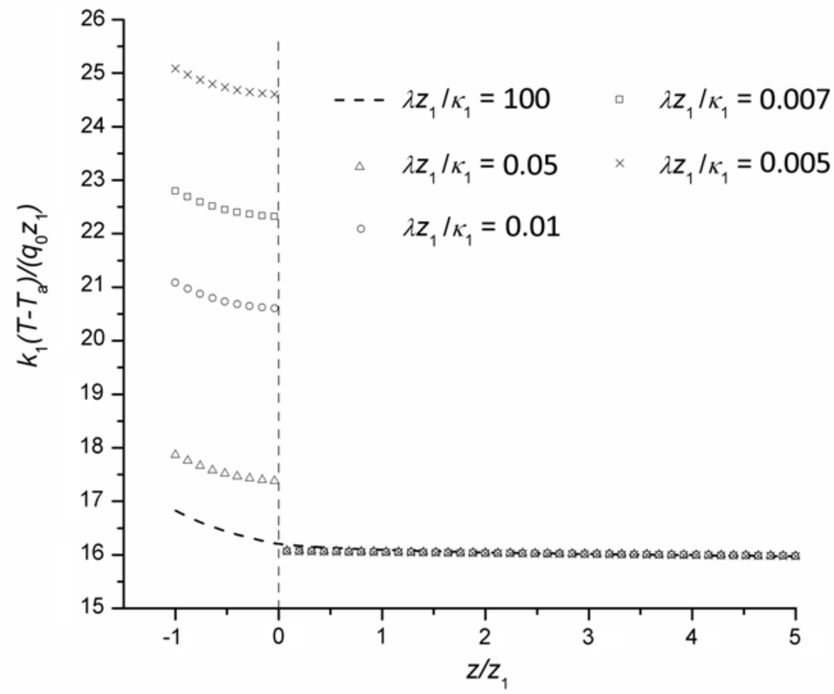

Figure 12. Plots of $\kappa_1(T - T_\mathrm{a})/(q_0 z_1)$ against z/z_1 for a few selected values of $\alpha/(\kappa_1 z_1)$ (for low conducting interfaces).

On the whole, Figures 11 and 12 summarize the effects of the three types of interfaces $-$ low conducting, perfectly conducting and high conducting ones $-$ on the thermal performance of the heat dissipation system in Figure 10.

5 Summary

Boundary element procedures based on special Green's functions are proposed for analyzing axisymmetric heat conduction across low conducting and high conducting interfaces between two dissimilar materials. As the Green's functions satisfy the relevant interfacial conditions, the boundary element procedures do not require the interfaces to be discretized into elements, giving rise to smaller systems of linear algebraic equations to be solved. The procedures are applied to solve particular problems with known exact solutions. The numerical solutions obtained confirm the validity of the Green's functions and the proposed Green's function boundary element procedures.

References

[1] Y. Benveniste, On the decay of end effects in conduction phenomena: a sandwich strip with imperfect interfaces of low or high conductivity, *Journal of Applied Physics* **86** (1999) 1273-1279.

[2] A. Desai, J. Geer, B. Sammakia, Models of steady heat conduction in multiple cylindrical domains, *Journal of Electronic Packaging-Transactions of the ASME* **128** (2006) 10-17.

[3] J. R. Berger, A. Karageorghis, The method of fundamental solutions for heat conduction in layered materials. *International Journal for Numerical Methods in Engineering* **45** (1999) 1681-1694.

[4] W. T. Ang, K. K. Choo, H. Fan, A Green's function for steady-state two-dimensional isotropic heat conduction across a homogeneously imperfect interface, *Communications in Numerical Methods in Engineering* **20** (2004) 391-399.

[5] W. T. Ang, Non-steady state heat conduction across an imperfect interface: a dual-reciprocity boundary element approach, *Engineering Analysis with Boundary Elements* **30** (2006) 781-789.

[6] X. Wang, L. J. Sudak, 3D Green's functions for a steady point heat source interacting with a homogeneous imperfect interface, *Journal of Mechanics of Materials and Structures* **1** (2006) 1269-1280.

[7] C. A. Brebbia, J. C. F. Telles, L. C. Wrobel, *Boundary Element Techniques, Theory and Applications in Engineering*, Springer-Verlag, Berlin/Heidelberg, 1984.

Appendix

With reference to a Cartesian coordinate system $Oxyz$, consider the half-spaces $z < 0$ and $z > 0$ being occupied by two dissimilar homogeneous materials having thermal conductivities κ_1 and κ_2 respectively. We derive here Green's functions for three-dimensional steady-state heat conduction across low and high conducting interfaces at $z = 0$.

The required Green's functions denoted by $\Phi(x, y, z; \xi, \eta, \zeta)$ are solutions of the partial differential equation

$$\frac{\partial^2\Phi}{\partial x^2} + \frac{\partial^2\Phi}{\partial y^2} + \frac{\partial^2\Phi}{\partial z^2} = \delta(x-\xi)\delta(y-\eta)\delta(z-\zeta), \tag{A1}$$

where δ denotes the Dirac-delta function.

Equation (A1) admits solutions of the form

$$\Phi(x, y, z; \xi, \eta, \zeta) = -\frac{H(z)H(\zeta) + H(-z)H(-\zeta)}{4\pi\sqrt{(x-\xi)^2 + (y-\eta)^2 + (z-\zeta)^2}} + \Phi^*(x, y, z; \xi, \eta, \zeta), \tag{A2}$$

where $\Phi^*(x, y, z; \xi, \eta, \zeta)$ is any solution of the partial differential equation

$$\frac{\partial^2\Phi^*}{\partial x^2} + \frac{\partial^2\Phi^*}{\partial y^2} + \frac{\partial^2\Phi^*}{\partial z^2} = 0. \tag{A3}$$

Note that $H(x)$ denotes the unit-step Heaviside function.

The function $\Phi^*(x,y,z;\xi,\eta,\zeta)$ are given in Wang and Sudak [6] for low and high conducting interfaces for $\zeta=0$. The analysis in [6] can be modified to include the case where $\zeta \neq 0$. We take $\Phi^*(x,y,z;\xi,\eta,\zeta)$ to be of the form

$$\begin{aligned}
& \Phi^*(x,y,z;\xi,\eta,\zeta) \\
= \; & H(-\zeta)\{H(-z)[\frac{a_0}{4\pi\sqrt{(x-\xi)^2+(y-\eta)^2+(z+\zeta)^2}} \\
& +a_1\int_0^\infty \frac{\exp(-a_3 u)du}{\sqrt{(x-\xi)^2+(y-\eta)^2+(z+\zeta-u)^2}}] \\
& +H(z)a_2\int_0^\infty \frac{\exp(-a_3 u)du}{\sqrt{(x-\xi)^2+(y-\eta)^2+(z-\zeta+u)^2}}\} \\
& +H(\zeta)\{H(z)[\frac{b_0}{4\pi\sqrt{(x-\xi)^2+(y-\eta)^2+(z+\zeta)^2}} \\
& +b_1\int_0^\infty \frac{\exp(-b_3 u)du}{\sqrt{(x-\xi)^2+(y-\eta)^2+(z+\zeta+u)^2}}] \\
& +H(-z)b_2\int_0^\infty \frac{\exp(-b_3 u)du}{\sqrt{(x-\xi)^2+(y-\eta)^2+(z-\zeta-u)^2}}\}, \qquad \text{(A4)}
\end{aligned}$$

where a_0, a_1, a_2, a_3, b_0, b_1, b_2 and b_3 are constants. We assume a priori that a_3 and b_3 are positive constants so that the improper integrals over $[0,\infty)$ in (A4) exist.

It may be easily verified that (A4) is a solution of (A3) at all points (x,y,z) in space. The constants a_0, a_1, a_2, a_3, b_0, b_1, b_2 and b_3 are chosen to satisfy the conditions on the interfacial conditions.

Low conducting interface

For the case in which $z=0$ is low conducting, $\Phi(x,y,z;\xi,\eta,\zeta)$ is required to satisfy the interfacial conditions

$$\kappa_1\frac{\partial}{\partial z}[\Phi(x,y,z;\xi,\eta,\zeta)]\bigg|_{z=0^-} = \kappa_2\frac{\partial}{\partial z}[\Phi(x,y,z;\xi,\eta,\zeta)]\bigg|_{z=0^+},$$

$$\lambda[\Phi(x,y,0^+;\xi,\eta,\zeta) - \Phi(x,y,0^-;\xi,\eta,\zeta)] = \kappa_2 \frac{\partial}{\partial z}[\Phi(x,y,z;\xi,\eta,\zeta)]\Big|_{z=0^+}. \tag{A5}$$

If we take $a_0 = b_0 = -1$, the condition on the first line of (A5) is satisfied if

$$\begin{aligned} -\kappa_1 a_1 &= \kappa_2 a_2, \\ -\kappa_1 b_2 &= \kappa_2 b_1. \end{aligned} \tag{A6}$$

For $\zeta < 0$, the condition on the second line of (A5) is satisfied if

$$\begin{aligned} &\lambda(a_2 - a_1)\int_0^\infty \frac{\exp(-a_3 u)du}{\sqrt{(x-\xi)^2 + (y-\eta)^2 + (u-\zeta)^2}} \\ &+\frac{\lambda}{2\pi\sqrt{(x-\xi)^2 + (y-\eta)^2 + \zeta^2}} \\ = \;& -\kappa_2 a_2 \int_0^\infty \frac{(u-\zeta)\exp(-a_3 u)du}{[(x-\xi)^2 + (y-\eta)^2 + (u-\zeta)^2]^{3/2}}. \end{aligned} \tag{A7}$$

Using the integration by parts, we obtain

$$\begin{aligned} &\int \frac{(u-\zeta)\exp(-a_3 u)du}{[(x-\xi)^2 + (y-\eta)^2 + (u-\zeta)^2]^{3/2}} \\ = \;& -\frac{\exp(-a_3 u)}{[(x-\xi)^2 + (y-\eta)^2 + (u-\zeta)^2]^{1/2}} \\ &-a_3 \int \frac{\exp(-a_3 u)du}{\sqrt{(x-\xi)^2 + (y-\eta)^2 + (u-\zeta)^2}}. \end{aligned} \tag{A8}$$

From (A7) and (A8), it follows that

$$\begin{aligned} -2\pi\kappa_2 a_2 &= \lambda, \\ \kappa_2 a_2 b_3 &= \lambda(a_2 - a_1). \end{aligned} \tag{A9}$$

Similarly, for $\zeta > 0$, we obtain

$$\begin{aligned} 2\pi\kappa_2 b_1 &= \lambda, \\ -\kappa_2 b_1 b_3 &= \lambda(-b_1 + b_2). \end{aligned} \tag{A10}$$

Solving (A6), (A9) and (A10) gives

$$\begin{aligned} a_1 &= -b_2 = \frac{\lambda}{2\pi\kappa_1}, \\ a_2 &= -b_1 = -\frac{\lambda}{2\pi\kappa_2}, \\ a_3 &= b_3 = \frac{\lambda}{\kappa_2}(1+\frac{\kappa_2}{\kappa_1}). \end{aligned} \tag{A11}$$

Note that a_3 and b_3 are positive (as assumed).

Thus, the required three-dimensional Green's function for the case in which the interface $z = 0$ is low conducting is given by (A2), (A4) and (A11).

High conducting interface

For the case in which $z = 0$ is high conducting, $\Phi(x, y, z; \xi, \eta, \zeta)$ is required to satisfy the interfacial conditions

$$\begin{aligned} &\Phi(x, y, 0^+; \xi, \eta, \zeta) = \Phi(x, y, 0^-; \xi, \eta, \zeta), \\ &\kappa_2 \frac{\partial}{\partial z}[\Phi(x, y, z; \xi, \eta, \zeta)]\bigg|_{z=0^+} - \kappa_1 \frac{\partial}{\partial z}[\Phi(x, y, z; \xi, \eta, \zeta)]\bigg|_{z=0^-} \\ = {} & \alpha \frac{\partial^2}{\partial z^2}[\Phi(x, y, z; \xi, \eta, \zeta)]\bigg|_{z=0}. \end{aligned} \tag{A12}$$

Taking $a_0 = b_0 = 1$, the condition on the first line of (A12) is satisfied if

$$\begin{aligned} a_1 &= a_2, \\ b_1 &= b_2. \end{aligned} \tag{A13}$$

For $\zeta < 0$, the condition on the second line of (A12) is satisfied if

$$\begin{aligned}
&-(\kappa_1 a_1 + \kappa_2 a_2) \int_0^\infty \frac{(u-\zeta)\exp(-a_3 u) du}{[(x-\xi)^2 + (y-\eta)^2 + (u-\zeta)^2]^{3/2}} \\
&\qquad + \frac{\kappa_1 \zeta}{2\pi[(x-\xi)^2 + (y-\eta)^2 + \zeta^2]^{3/2}} \\
= \;& \alpha a_2 \int_0^\infty \exp(-a_3 u) \frac{\partial^2}{\partial z^2}[\frac{1}{\sqrt{(x-\xi)^2 + (y-\eta)^2 + (u-\zeta)^2}}]\Bigg|_{z=0} du.
\end{aligned} \tag{A14}$$

Using integration by parts and the relation

$$\begin{aligned}
&\frac{\partial^2}{\partial z^2}[\frac{1}{\sqrt{(x-\xi)^2 + (y-\eta)^2 + (z-\zeta+u)^2}}]\Bigg|_{z=0} \\
= \;& \frac{\partial^2}{\partial u^2}[\frac{1}{\sqrt{(x-\xi)^2 + (y-\eta)^2 + (u-\zeta)^2}}],
\end{aligned} \tag{A15}$$

we obtain

$$\begin{aligned}
&\frac{\kappa_1 \zeta}{2\pi[(x-\xi)^2 + (y-\eta)^2 + \zeta^2]^{3/2}} - \frac{(\kappa_1 a_1 + \kappa_2 a_2)}{\sqrt{(x-\xi)^2 + (y-\eta)^2 + \zeta^2}} \\
&+ a_3(\kappa_1 a_1 + \kappa_2 a_2) \int_0^\infty \frac{\exp(-a_3 u) du}{\sqrt{(x-\xi)^2 + (y-\eta)^2 + (u-\zeta)^2}} \\
= \;& \alpha a_2 \{ -\frac{\zeta}{[(x-\xi)^2 + (y-\eta)^2 + \zeta^2]^{3/2}} - \frac{a_3}{\sqrt{(x-\xi)^2 + (y-\eta)^2 + \zeta^2}} \\
&+ a_3^2 \int_0^\infty \frac{\exp(-a_3 u) du}{\sqrt{(x-\xi)^2 + (y-\eta)^2 + (u-\zeta)^2}} \}.
\end{aligned} \tag{A16}$$

From (A16), it follows that

$$\begin{aligned}
\kappa_1 &= -2\pi\alpha a_2, \\
(\kappa_1 a_1 + \kappa_2 a_2) &= \alpha a_2 a_3.
\end{aligned} \tag{A17}$$

Similarly, for $\zeta > 0$, we obtain

$$\begin{aligned} \kappa_2 &= -2\pi\alpha b_2, \\ (\kappa_1 b_2 + \kappa_2 b_1) &= \alpha b_2 b_3. \end{aligned} \tag{A18}$$

Solving (A13), (A17) and (A18) gives

$$\begin{aligned} a_1 &= a_2 = -\frac{\kappa_1}{2\pi\alpha}, \\ b_1 &= b_2 = -\frac{\kappa_2}{2\pi\alpha}, \\ a_3 &= b_3 = \frac{1}{\alpha}(\kappa_1 + \kappa_2). \end{aligned} \tag{A19}$$

Note that a_3 and b_3 are positive (as assumed).

Thus, the required three-dimensional Green's function for the case in which the interface $z = 0$ is high conducting is given by (A2), (A4) and (A19).